Spectra of Noise and Amplified Turbulence Emanating from Shock-Turbulence Interaction

Herbert S. Ribner*
University of Toronto, Downsview, Ontario, Canada
and
NASA Langley Research Center, Hampton, Virginia

This work is a small extension of our NACA studies of the early 1950's that predicted amplification of turbulence on passing through a shock wave (observed for turbulent boundary layers), as well as the generation of intense noise (observed for supersonic jets). There is a brief review of aspects of the basic theory: 1) the interaction of an infinite planar shock with a single three-dimensional spectrum component of turbulence (an oblique sinusoidal "shear wave"); and 2) parts of the three-dimensional spectrum analysis necessary to generalize the scenario to the interaction of a shock wave with convected homogeneous turbulence. The original calculations yielded curves vs Mach number of rms sound pressure, temperature fluctuation, and two components of turbulent velocity downstream of the shock; those for isotropic preshock turbulence (arbitrary spectrum) are reproduced herein. For the particular case of the von Kármán three-dimensional spectrum the present study provides, in addition, the one-dimensional power spectra (vs wavenumber or frequency) of these quantities. Ratios of the several postshock spectra to the longitudinal preshock turbulence spectrum (one-dimensional) are presented graphically for a wide range of Mach numbers.

Nomenclature

$\tilde{a}$ = 1.3390, pure number
$\tilde{B}$ = $55/(18\pi\tilde{a})$, pure number
c_A, c = pre- and postshock sound speeds, respectively
c^* = critical sound speed
$\boldsymbol{K}$ = nondimensional wavenumber vector [K_1, K_2, K_3 or K, $\theta+(\pi/2)$, ϕ, Fig. 1; also K_r K_1, $\theta+(\pi/2)$, Fig. 2]
k = $k/\tilde{a}L$, actual wavenumber vector
L = longitudinal scale of turbulence
M = U_A/c_A, preshock Mach number
M_1 = U/c, postshock Mach number
P = transfer function relating dp'' to du
$\hat{P}$ = ambient pressure
p'' = pressure perturbation
T = transfer function relating $d\tau'$ to du
$\hat{T}$ = ambient temperature
r, ϕ, X_1 = cylindrical coordinates for components of $\boldsymbol{K}$ and dZ
U_A, U = pre- and postshock stream velocity, respectively
u, v, w = nondimensional components of velocity perturbation in directions X_1, X_2, X_3, respectively (actual components/c^*)
X = nondimensional field point vector (X_1, X_2, X_3), Fig. 1; X_1 is $\perp$ shock
x = $X\tilde{a}L$, actual field point vector
$\tilde{X}$ = transfer function relating du' to du
dZ_σ = (complex) wave amplitude associated with $\sigma = u, r, \phi, \tau', p''$, etc.
γ = ratio of specific heats (taken as 1.4)
θ = polar angle of dZ; $\theta+(\pi/2)$ = polar angle of $\boldsymbol{K}$ (Figs. 1-3)
θ_{cr} = critical angle separating evanescent and nonevanescent pressure waves
ρ_A, ρ = pre- and postshock fluid density, respectively
τ' = temperature perturbation
ϕ = azimuth angle of $\boldsymbol{K}$ (Figs. 1 and 2)
Φ_σ = one-dimensional spectral density associated with $\sigma = u, v, u', \tau', p''$, etc.
ω = radian frequency ($2\pi \times$ frequency)

Superscript

$\hat{(\ )}$ = actual dimensional quantity

Received Dec. 6, 1985; revision received June 12, 1986.

*Professor, Institute for Aerospace Studies, Toronto; also Distinguished Research Associate, NASA Langley.

Introduction

ANALYTICAL studies of three-dimensional disturbances convected through, and interacting with, a shock wave seem to have commenced in the early 1950's.[1-4] The disturbances were waves of 1) vorticity, 2) entropy, or 3) sound; they were in the form of oblique planar, usually sinusoidal, patterns. Any one such wave encountering the shock would generate all three kinds on the downstream side. It was pointed out by Ribner[1,5,6] and by Batchelor[7] that the vorticity waves (called therein "shear waves") were three-dimensional Fourier components of arbitrary incompressible flows, e.g., weak turbulence (see also Moyal[8]).

The initial papers[1-4] treated the interaction of individual waves of arbitrary inclination with an infinite plane shock; the analyses were linearized in terms of wave amplitude. A later paper[6] developed the comprehensive three-dimensional spectrum analysis necessary to describe the interaction of turbulence with a shock; the earlier single-wave results were the "building blocks." Calculations were carried out for rms values of turbulence velocity components, temperature, and pressure (sound) fluctuations downstream of the shock, assuming either isotropic or axisymmetric preshock turbulence. The plotted curves showed that velocity components of the postshock turbulence would be amplified as much as 45% relative to preshock levels. Recent measurements do display the phenomenon of amplification (e.g., Refs. 9 and 10).

The calculation of such *turbulence amplification* on passage through a shock has received renewed attention in

recent years.[11-13] The term "turbulence" in this context is, however, a misnomer: these papers have reverted to dealing with a single three-dimensional spectral component of turbulence. They oversimplify in interpreting the single-wave results as representative of the broad spectrum of waves constituting turbulence. On the other hand, two of them[12,13] pioneer in the application of numerical integration of the Euler equations to the single-wave shock-interaction problem. By coping with nonlinearity, they test the range of applicability of the results of the linear analysis.

Some other studies based on the same fluid dynamics, but quite distinct in orientation, may be noted. These relate to the passage of a columnar vortex broadside through a planar shock wave: a cylindrical sound wave appears on the downstream side, partly cut off by the shock, as well as a modified vortex. The single-wave (single Fourier component) results of, e.g., Ref. 1, can serve as the "building blocks" to compute this sound wave in detail.[14,15] Unlike the shock-turbulence interaction problem, which is stochastic, this phenomenon is deterministic (and is more readily verifiable by experiment[16,17]). Nevertheless, the underlying analytical framework is the same. Both problems have been considered relevant to the generation of "shock noise" by turbulence passing through the shock pattern of a supersonic jet.[6,15,18]

It appears then that, despite other results both old and new, the only genuine calculations of turbulence interacting with a shock wave are those of the early Ref. 6. But these, as noted previously, have been limited to rms values of the relevant disturbances: there are no computed spectra. The present study is an extension of that paper in a very limited sense; it seeks to provide the one-dimensional power spectra (vs wave number or frequency) of velocity, temperature, and pressure perturbations. The procedure is one of numerical integration of the corresponding three-dimensional spectra. These are adapted from Ref. 6 with the three-dimensional spectrum of the preshock turbulence specified.

Shock-Turbulence Interaction

Transfer Functions Connecting Fourier Components (Deterministic)

A snapshot of an arbitrary flowfield may be represented by a Fourier-Stieltjes integral in three dimensions as

$$u(X)=\int du=\int dZ_u(\boldsymbol{K})\exp(i\boldsymbol{K}\cdot\boldsymbol{X});\quad \boldsymbol{K}=K_1,K_2,K_3$$

$$v(X)=\int dv=\int dZ_v(\boldsymbol{K})\exp(i\boldsymbol{K}\cdot\boldsymbol{X});\quad |\boldsymbol{K}|\equiv K=2\pi/\text{wavelength}$$

$$w(X)=\int dw=\int dZ_w(\boldsymbol{K})\exp(i\boldsymbol{K}\cdot\boldsymbol{X});\quad X=X_1,X_2,X_3 \tag{1}$$

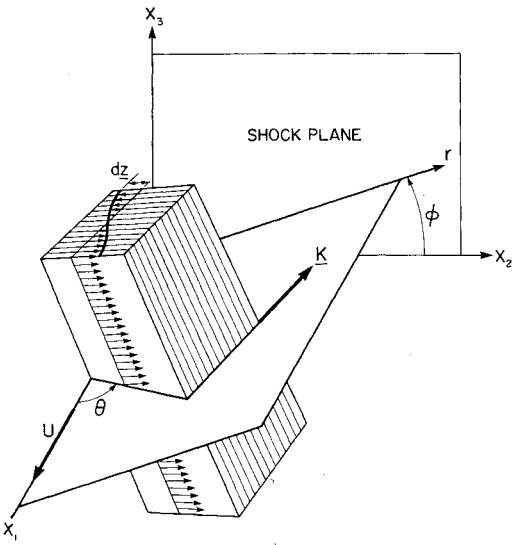

Fig. 1 Perspective view of shear wave (three-dimensional spectral component of turbulence) in relation to reference frame. Note that dZ is not in general in the plane of K and U.

This integral is effectively a superposition of plane sinusoidal waves with wavenumber $\boldsymbol{K}$ normal to the planes of constant phase; variation of $\boldsymbol{K}$ implies a distribution of wavelengths and *orientations*. We can apply this format to weak, essentially "frozen" turbulence (a pattern with negligible time dependence); this will behave almost incompressibly, governed by

$$\frac{\partial u}{\partial X_1}+\frac{\partial v}{\partial X_2}+\frac{\partial w}{\partial X_3}=0 \tag{2}$$

even though convected at high speed. Applying this constraint to Eq. (1a) shows that the amplitude dZ and wavenumber $\boldsymbol{K}$ are orthogonal:

$$K_1dZ_u+K_2dZ_v+K_3dZ_w=\boldsymbol{K}\cdot d\boldsymbol{Z}=0;\quad d\boldsymbol{Z}=dZ_u,dZ_v,dZ_w \tag{3}$$

Thus an individual wave is transverse; it may be interpreted physically as an oblique sinusoidal wave of shearing motion (Fig. 1).

Such a wave, when convected into a shock, interacts in a predictable fashion according to linear theory[1-4]: a "refracted" shear wave, a superposed entropy wave, and a pressure wave emerge on the downstream side. If the initial pattern of waves (upstream turbulence) is known only statistically, then the downstream pattern (modified turbulence, entropy "spottiness," and noise) can be determined statistically. That is, spectra, correlations, and mean square values can be calculated.

To this end, we incorporated the deterministic single-wave relations[1] into a comprehensive spectrum analysis in three dimensions[6] for homogeneous turbulence. A brief account of relevant parts of the development is given below. The physical quantities are normalized so as to be *nondimensional*: u,v,w, etc. = velocity components/critical sound speed c^*; p'' = pressure perturbation/ambient $\hat{P}$, and τ' = temperature perturbation/ambient $\hat{T}$. (But addition of a superscript ($\hat{}$) to u, p'', τ', etc., removes the normalization.)

It will be convenient to re-express the velocity field of an incident plane shear wave (Fig. 1) in cylindrical coordinates as (see also Fig. 2 where the wave is viewed edge-on)

$$(du,dv_r,dv_\phi)=(dZ_u,dZ_r,dZ_\phi)\exp(i\boldsymbol{K}\cdot\boldsymbol{X}) \tag{4}$$

where du is parallel to X_1 (normal to the shock), dv_r is parallel to r, and dv_ϕ is perpendicular to r and X_1 in the direction of increasing ϕ. The planes of constant phase $\boldsymbol{K}\cdot\boldsymbol{X}$ ($=\boldsymbol{k}\cdot\boldsymbol{x}$, see below) = const make an angle θ with the X_1 axis. Herein the wavenumber $\boldsymbol{K}$ and position vector $\boldsymbol{X}$ are nondimensional; they are formed from their dimensional counterparts $\boldsymbol{k}$ and $\boldsymbol{x}$ as

$$\boldsymbol{K}=k\tilde{a}L;\qquad L=\text{turbulence longitudinal scale}$$

$$\boldsymbol{X}=\boldsymbol{x}/\tilde{a}L;\qquad \tilde{a}=\text{pure number} \tag{5}$$

respectively.

Figure 3 shows the results of the encounter of the incident wave, Eq. (4), with the shock. The three waves that appear on the downstream side are as follows:

Refracted shear wave, with X_1 component (other components are of no concern here)

$$du'=dZ_u'(\boldsymbol{K}')\exp(i\boldsymbol{K}'\cdot\boldsymbol{X});\qquad dZ_u'=\tilde{X}dZ_u \tag{6}$$

Entropy wave, aligned with refracted shear wave

$$d\tau'=dZ_\tau'(\boldsymbol{K}')\exp(i\boldsymbol{K}'\cdot\boldsymbol{X});\qquad dZ_\tau'=TdZ_u \tag{7}$$

Sound wave

$$dp'' = dZ_p''(\boldsymbol{K}'')\exp(i\boldsymbol{K}''\cdot\boldsymbol{X}); \qquad dZ_p'' = P\,dZ_u \tag{8}$$

The planes of constant phase $\boldsymbol{K}'\cdot\boldsymbol{X}=$ const and $\boldsymbol{K}''\cdot\boldsymbol{X}=$ const make angles θ' and θ'', respectively, with the X_1 axis or shock normal (Fig. 3). These angles are functions of the angle θ of the incident wave (and of the Mach number). For $|\theta|$ in the range from zero to a critical value θ_{cr}, the pressure wave decays exponentially with distance from the shock (in proportion to wave number): such waves are called "evanescent." For $|\theta|$ in the range from θ_{cr} to $\pi/2$, the wave shows no decay and is called "nonevanescent" herein.

The right-hand set of equations relates the respective amplitudes of the downstream wave components with that of the initial longitudinal shear wave component dZ_u. The *transfer functions* $\tilde{X}$, T, and P are all dependent on the incident wave angle θ, as well as Mach number M; they are the results of a gasdynamic analysis carried out in Ref. 1. Functional expressions, taken or adapted thereform, are given in Appendix A. The transfer functions are quite different in the regimes 0 to θ_{cr} and θ_{cr} to $\pi/2$; in particular, the form of P dictates evanescence in the former and nonevanescence in the latter.

Three-Dimensional and One-Dimensional Power Spectra (Stochastic)

For application to a stochastic field such as turbulence, it is necessary to go over to statistical relations. If we form an ensemble average for waves of different wavenumbers $\boldsymbol{K}$ and $\boldsymbol{\kappa}$ in respective ranges $d^3\boldsymbol{K}$ and $d^3\boldsymbol{\kappa}$, it is easily proved that

$$\overline{dZ_u(\boldsymbol{K})\,dZ_u^*(\boldsymbol{\kappa})} = [uu]\,\delta(\boldsymbol{\kappa}-\boldsymbol{K})\,d^3\boldsymbol{K}\,d^3\boldsymbol{\kappa} \tag{9}$$

if the turbulence is homogeneous.[8,19] The quantity $[uu]$ is a special symbol for the three-dimensional spectral density of $\overline{u^2}$ in wavenumber space $\boldsymbol{K}$. The vanishing of $\delta(\boldsymbol{\kappa}-\boldsymbol{K})$ for $\boldsymbol{\kappa}\neq\boldsymbol{K}$ implies that waves of different wavelengths or inclinations (since $\boldsymbol{\kappa}$ and $\boldsymbol{K}$ are vectors) are statistically independent.

The integral of Eq. (9) over $\boldsymbol{\kappa}$ space may be written, by virtue of the δ function, as

$$\overline{dZ_u(\boldsymbol{K})\,dZ_u^*(\boldsymbol{K})} = [uu]\,d^3\boldsymbol{K} \tag{10}$$

In similar fashion, we can develop corresponding expressions for the three-dimensional spectra $[u'u']$, $[\tau'\tau']$, $[p''p'']$, etc. The integral of Eq. (10) over $\boldsymbol{K}$ space is $\overline{u^2}$, that of $[\tau'\tau']$ over $\boldsymbol{K}'$ space is $\overline{\tau'^2}$, and so on.

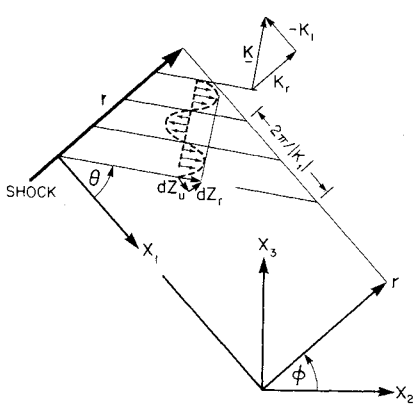

Fig. 2 Projective view of shear wave in relation to reference frame.

Application of these procedures to Eqs. (6–8) leads to[6]

$$\begin{aligned}
\overline{u^2} &= \iiint [uu]\,d^3\boldsymbol{K} \\
\overline{u'^2} &= \iiint [u'u']\,d^3\boldsymbol{K}' = \iiint |\tilde{X}|^2\,[uu]\,d^3\boldsymbol{K} \\
\overline{\tau'^2} &= \iiint [\tau'\tau']\,d^3\boldsymbol{K}' = \iiint |T|^2\,[uu]\,d^3\boldsymbol{K} \\
\overline{p''^2} &= \iiint [p''p'']\,d^3\boldsymbol{K}'' = \iiint |P|^2\,[uu]\,d^3\boldsymbol{K}
\end{aligned} \tag{11}$$

where the integration limits are $\pm\infty$ in K_1, K_2, K_3.

We shall limit attention to axisymmetric turbulence, with main emphasis on the special case of isotropy. This and the axisymmetry of the shock interaction process led us in the earlier material[6] to employ cylindrical coordinates. In these coordinates,

$$d^3\boldsymbol{K} = d\phi\,K_r\,dK_r\,dK_1 \tag{12}$$

A first integration with respect to $d\phi$ then yields a factor 2π, so that

$$\begin{aligned}
\overline{u^2} &= 2\pi\int_{-\infty}^{\infty}\int_0^{\infty} [uu]\,K_r\,dK_r\,dK_1 \equiv \int_{-\infty}^{\infty} \Phi_u(K_1)\,dK_1 \\
\overline{u'^2} &= 2\pi\int_{-\infty}^{\infty}\int_0^{\infty} |\tilde{X}|^2\,[uu]\,K_r\,dK_r\,dK_1 \equiv \int_{-\infty}^{\infty} \Phi_{u'}(K_1)\,dK_1 \\
\overline{\tau'^2} &= 2\pi\int_{-\infty}^{\infty}\int_0^{\infty} |T|^2\,[uu]\,K_r\,dK_r\,dK_1 \equiv \int_{-\infty}^{\infty} \Phi_{\tau'}(K_1)\,dK_1 \\
\overline{p''^2} &= 2\pi\int_{-\infty}^{\infty}\int_0^{\infty} |P|^2\,[uu]\,K_r\,dK_r\,dK_1 \equiv \int_{-\infty}^{\infty} \Phi_{p''}(K_1)\,dK_1
\end{aligned} \tag{13}$$

respectively.

The one-dimensional spectra Φ_u, $\Phi_{u'}$, $\Phi_{\tau'}$, and $\Phi_{p''}$ are effectively defined in Eqs. (13) in terms of integrals over K_r; these involve the longitudinal three-dimensional power spectral density $[uu]$ and the respective transfer functions 1, $\tilde{X}$, T, P that quantify the shock interaction process. As formulated, all four spectra are functions of the *preshock* longitudinal wavenumber K_1. This is convenient and puts them on a common basis. Moreover, K_1 is proportional to radian frequency ω in the form

$$K_1 = \omega\tilde{a}L/U_A \tag{14}$$

[This follows from $k_1 = \omega/U_A$ and the definition, Eq. (5), connecting the two k's.]

Although the interaction process of Fig. 3 conserves K_r but *not* K_1, $(K_1 \neq K_1' \neq K_1'')$, the frequency ω is invariant $(\omega=\omega'=\omega'')$. That is, an observer perceives the same frequency as each of the wave patterns moves past. This is, of

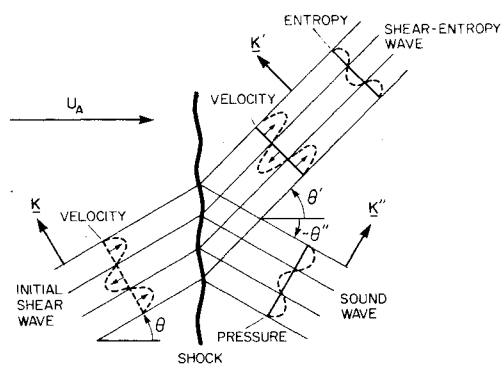

Fig. 3 Interaction of shear wave and shock. View in X_1, r plane.

course, a necessary result for a statistically steady process. A geometric analysis formally confirms the invariance of ω.

Isotropic Preshock Turbulence

For evaluation of the one-dimensional spectra of Eqs. (13), the three-dimensional longitudinal spectrum $[uu]$ of the input turbulence must be specified. The von Kármán spectral model (called θ_{11} in Ref. 20) is chosen; in our notation it is

$$[uu] = \overline{u^2}\,\frac{\tilde{B}K_r^2}{2\pi[1+K_1^2+K_r^2]^{17/6}} \tag{15}$$

$$\tilde{B} = 55/(18\pi\tilde{a}), \qquad \tilde{a} = 1.3390$$

where the longitudinal scale L of the turbulence is incorporated in $K = k\tilde{a}L$. The pure number $\tilde{a}$ is a normalizing constant chosen so that

$$\int_{-\infty}^{\infty} dK_1 \int_0^{\infty} [uu]\,2\pi K_r dK_r = \overline{u^2} \tag{16}$$

For numerical evaluation of the one-dimensional spectra, it will be convenient to express the cylindrical wavenumber component K_r in terms of the longitudinal component K_1 and the polar angle $\theta+\pi/2$. This will replace the infinite range in K_r by a finite range in θ. It will also be easier to interpret the integral in terms of the geometry of Fig. 3. Following Ref. 6 [Eq. (56)], we put (Figs. 1 and 2)

$$K_1 = -K\sin\theta, \qquad K_2 = K\cos\theta\cos\phi$$

$$K_3 = K\cos\theta\sin\phi, \qquad K_r = \sqrt{K_2^2+K_3^2} = |K_1|\cot\theta$$

$$dK_r = |K_1|\csc^2\theta d\theta \tag{17}$$

Inserting Eqs. (15) and (17) into Eqs. (13) gives, after some reduction, the following format for evaluation of the one-dimensional spectra:

$$\frac{\Phi_1(K_1)}{\overline{u^2}} = \frac{\tilde{B}}{K_1^{5/3}} \int_0^{\pi/2} |\Gamma_i|^2 \frac{\cos^3\theta d\theta}{\sin^5\theta[b'+\cot^2\theta]^{17/6}} \tag{18}$$

where

$$b' = (1+K_1^2)/K_1^2$$

and

$$\text{for } i = u, u', \tau', p'', \qquad \Gamma_i = 1, \tilde{X}T, P$$

These express the general form to be integrated numerically for the shock interaction products in the present case, namely, isotropic preshock turbulence with statistics described by the von Kármán three-dimensional spectrum.

One-Dimensional Spectra of $\overline{v^2}$ and $\overline{v'^2}$

The one-dimensional power spectra of the cross-stream component velocity on the two sides of the shock involve a less straightforward derivation. An analysis and corresponding one-dimensional spectra of $\overline{v^2}$ and $\overline{v'^2}$ computed therefrom are given in Ref. 21; also treated there, are several other topics not included here for lack of space.

One-Dimensional Spectral Ratios: Lack of Uniqueness

The component of turbulent velocity normal to the shock, called u herein, has a central role in the analysis. The three-dimensional spectrum of $\overline{u^2}$ governs the shock interaction effects, and the resulting one-dimensional spectra are conveniently scaled to $\overline{u^2}$. Suppose, however, that we scale these one-dimensional spectra to the one-dimensional spectrum of $\overline{u^2}$: then this *ratio* in each case may be regarded as a sort of "power spectrum" transfer function; it will be a function of K_1. These quantities have been evaluated here only for the von Kármán three-dimensional preshock spectrum, a particular case of isotropic turbulence. The question may now be asked, how much will these spectral *ratios* change with changes in the preshock spectrum? For lack of space, this question is passed over here; the interested reader is referred to Ref. 21 for a comparative calculation based on axisymmetric preshock turbulence.

Results and Discussion

Rms Values of Postshock Disturbances, and Noise in Decibels

Figure 4 gives the variation with upstream Mach number of the various shock interaction products for a specific scenario: the preshock turbulence is isotropic with an intensity of 1% of freestream. The curves display rms perturbations of longitudinal velocity u and lateral velocity v or w in percent of initial stream velocity, and of rms temperature and pressure (noise) in percent of ambient. The figure is adapted from Fig. 4 of Ref. 6. The curves represent, in effect, the integrals with respect to K_1 of the respective one-dimensional spectra, that is, the integrals displayed in Eqs. (13). (The actual procedure, however, bypassed the one-dimensional spectra and employed only the specification of preshock isotropy. The results are independent of the preshock spectra, three- or one-dimensional, so long as they are consistent with isotropy.)

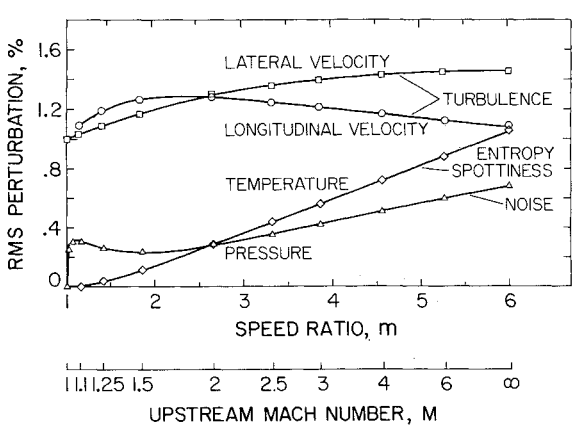

Fig. 4 Amplified turbulence and other disturbances produced downstream of shock by interaction with isotropic turbulence. Preshock turbulence intensity 1%. Rms velocities in percent of initial stream velocity; rms temperature and pressure (noise) in percent of ambient.

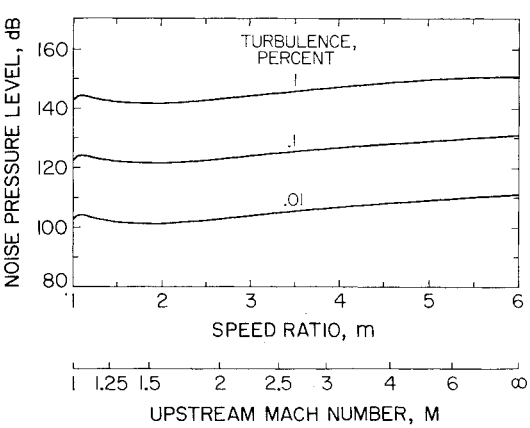

Fig. 5 Noise generated by shock-turbulence interaction (isotropic turbulence) on a decibel scale. Postshock ambient pressure, 1 atm.

The amplification of both the longitudinal and lateral components of the postshock turbulence is evident; it reaches some 45%, as noted in the Introduction, for the lateral component at high Mach number. The other two curves in Fig. 4 refer to the temperature and pressure fluctuations, respectively. (These are both spatial and temporal: rms values are the same from either point of view.) In first-order, these are absent from the postulated upstream flows. (Extremely weak second-order pressure and isentropic temperature fluctuations are associated with the specified 1% preshock turbulence.)

On an acoustical basis, the pressure fluctuation (noise) generated by the shock-turbulence interaction is very intense. This is shown in Fig. 5, where the noise level in decibels corresponding to Fig. 4 is plotted vs Mach number. The definition is

$$\mathrm{dB} = 20\log_{10}(\sqrt{\overline{p''^2}}/\hat{P}_{\mathrm{ref}}); \qquad \hat{P}_{\mathrm{ref}} = 2\times 10^{-10}\mathrm{atm} \qquad (19)$$

when the postshock ambient pressure is taken as 1 atm. For 1% preshock turbulence, the postshock noise level is predicted to exceed 140 dB for all preshock Mach numbers above 1.05.

One-Dimensional Spectra

Figure 6 displays normalized (nondimensional) one-dimensional power spectra calculated from the equations presented herein; the scenario is isotropic turbulence, governed by the von Kármán three-dimensional spectrum, being convected by an $M=1.25$ flow into a normal shock. The five spectra are

$\hat{\Phi}_u(K_1)/\overline{\hat{u}^2}$	longitudinal component of preshock turbulence
$\hat{\Phi}_{u'}(K_1)/\overline{\hat{u}^2}$	longitudinal component of postshock turbulence
$\hat{\Phi}_{\tau'}(K_1)/\hat{T}^2$	temperature fluctuation
$[\hat{\Phi}_{p''}(K_1)/\hat{P}^2]_{X=0}$	pressure fluctuation just downstream of shock (acoustic near field)
$[\hat{\Phi}_{p''}(K_1)/\hat{P}^2]_{X=\infty}$	pressure fluctuation far downstream of shock (acoustic far field)

The pressure field (noise) decays from an extremely high value just downstream of the shock ($X=0$) to an asymptotic lower value (still very intense acoustically) far downstream ($X=\infty$). Figure 6 shows a major difference in their spectral content: the $X=0$ near field is dominated by low frequencies, decaying asymptotically like $K_1^{-5/3}$ beyond $K_1\cong 3$. The $X=\infty$ far field is very deficient in low frequencies; on a linear scale it has a bell-shaped spectrum, peaking near $K_1=1$, but with the same asymptotic decay (the Kolmogorov $K_1^{-5/3}$ law) beyond $K_1\cong 3$.

Postshock/Preshock Spectral Ratios

Figure 6 applies for $M=1.25$; a series of such figures could be presented for a wide range of Mach numbers. A much neater alternative, however, is to take the *ratio* of each of these spectra at each value of K_1 to the $\Phi_u/\overline{u^2}$ spectrum. This ratio, as has been mentioned earlier, could be regarded as a sort of transfer function connecting the pair of spectra. In this format, the variation with Mach number can be discerned much more systematically.

Figure 7 presents such spectral ratios: it relates the postshock to the preshock longitudinal component of turbulence (the $\overline{u^2}$ divisors cancel) for a series of Mach numbers M. For convenience, the curves are normalized by factors $Z(M)$ (tabulated on the figure) to force agreement with the

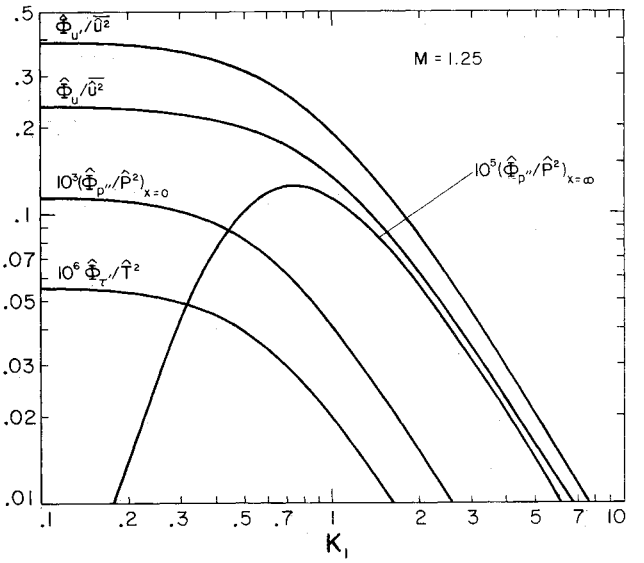

Fig. 6 Normalized one-dimensional power spectra of some of the shock interaction products whose rms values are given in Fig. 4, plus one other (see text). Mach number $M=1.25$ only.

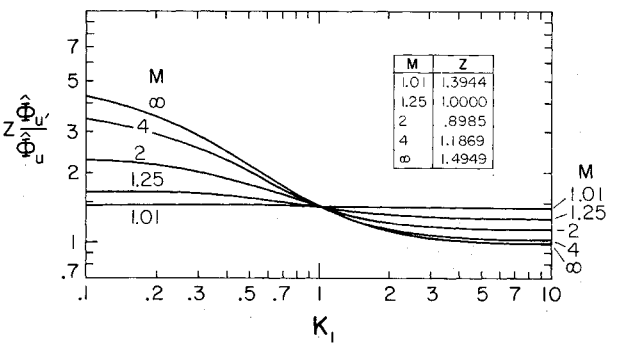

Fig. 7 Ratio of one-dimensional spectra for isotropic preshock turbulence: postshock longitudinal component/preshock longitudinal component.

$M=1.25$ curve at $K_1=1$; this makes the family of curves much more compact. It is seen that increasing Mach number enhances the low frequencies of the longitudinal component of the postshock turbulence.

Figure 8 gives the spectral ratios relating postshock temperature fluctuation (arising from entropy "spottiness" generated at the shock) to preshock longitudinal component of turbulence. It is evident that the low frequencies in the temperature field are somewhat enhanced compared with those of the turbulence field. The variation is not, however, monotonic with Mach number: there is a foldover of the curves with increasing M.

Figures 9 and 10 give the spectral ratios relating the near field and far field pressure fluctuations (noise), respectively, to the longitudinal component of the preshock turbulence. Here again, as in Fig. 6, it is seen that above $M\cong 1.25$ the acoustic far field is very deficient in low wavenumber content; that is, the shock-turbulence interaction process, although an extremely powerful noise generator overall (Fig. 5), is, except for weak shocks, relatively inefficient at low frequencies.

We conclude with a caveat concerning application of the present theory in the weak shock or low supersonic M region. Validity will be limited to correspondingly weak turbulence such that the linearized shock jump conditions used in this type of analysis[1-4] are not violated.

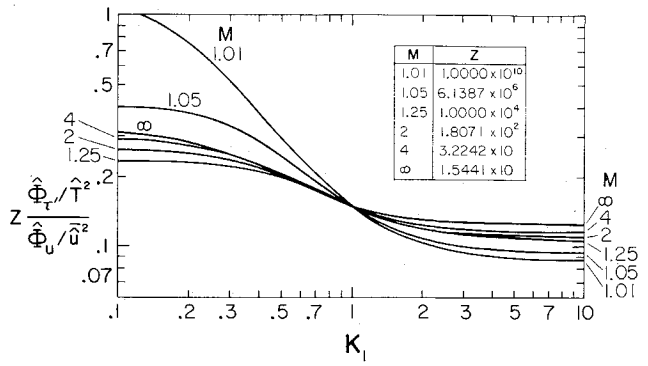

Fig. 8 Ratio of one-dimensional spectra for isotropic preshock turbulence: postshock temperature fluctuation/preshock longitudinal component of turbulence (both normalized).

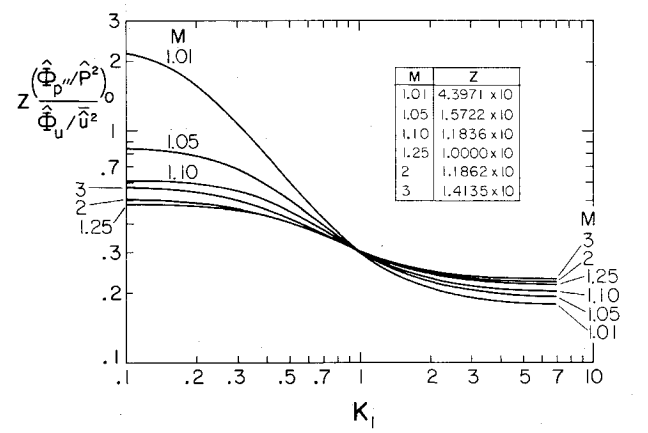

Fig. 9 Ratio of one-dimensional spectra for isotropic preshock turbulence: near field noise ($X=0$)/preshock longitudinal component of turbulence (both normalized).

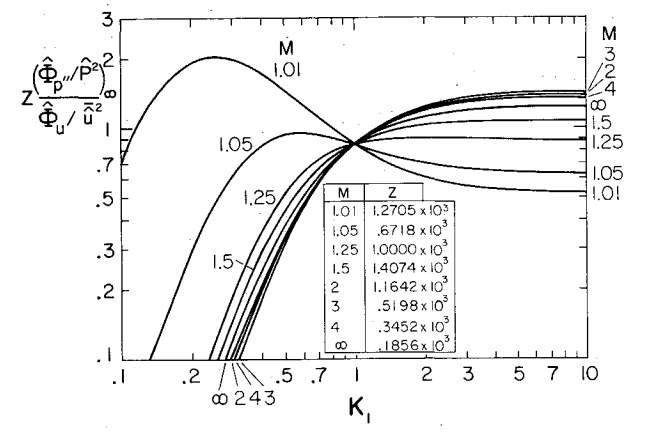

Fig. 10 Ratio of one-dimensional spectra for isotropic preshock turbulence: postshock far field noise ($X=\infty$)/preshock longitudinal component of turbulence (both normalized).

Appendix A: General Relations and Transfer Functions

The upstream (preshock) Mach number M and the incident wave inclination θ (Figs. 1-3) are specified. These dictate a virtual Mach number $\bar{W}$. A number of general relations are independent of the magnitude of $\bar{W}$; the remainder, notably the transfer functions, take different functional forms, depending on whether $\bar{W}<1$ or >1. The ratio of specific heats γ is taken as 1.4. (For formulas in terms of γ, see Ref. 6.)

General Relations

M = specified

$m = 6M^2/(M^2+5)$

$M_1 = \sqrt{(M^2+5)/(7M^2-1)}$

θ = specified

$\theta' = \tan^{-1}(m\tan\theta)$

$\bar{W} = M_1/\cos\theta'$

$\beta^2 = 1-M^2$

$\beta_w = \sqrt{|1-\bar{W}^2|}$

$\mu = \tan^{-1}(1/\beta_w)$

$\theta'_{cr} = \cos^{-1}M_1$

$\theta_{cr} = \cot^{-1}(m\cot\theta'_{cr})$

$\theta''_{cr} = \theta'_{cr} - \pi/2$

$\theta'' = -\tan^{-1}[M_1^2\tan\theta'/\beta^2]$ for $\bar{W}\le 1$

$= \theta' - \mu$ for $\bar{W}\ge 1$

Transfer Functions

$W\le 1 (0\le\lvert\theta\rvert\le\theta_{cr})$	$W\ge 1 (\theta_{cr}\le\lvert\theta\rvert\le\pi/2)$
$P = -\dfrac{2.8\Pi\sqrt{m}}{(2.4m-0.4)\cos\theta\cos\theta'}\times e^{i\delta_p}$	P = no change (n.c.)
$\Pi = \dfrac{(\cos\theta)}{m}\dfrac{\sqrt{c^2+d^2}}{\beta}\times e^{-K_r X\beta_\omega/\beta^2}$	$\Pi = \dfrac{\cos\theta\sin\mu}{m\cos\theta''}c$
$T = \sqrt{(a\tan\theta-1)^2+(b\tan\theta)^2}\times[0.8(m-1)^2 \div[(2.4m-0.4)\sqrt{m}]]e^{i\delta_T}$	T = n.c., with $b=0$
$\delta_s = \tan^{-1}(-B/A)$	$\delta_s = 0$
$\delta_T = \tan^{-1}[b/(\cot\theta-a)]$	$\delta_T = 0$
$\delta_p = \tan^{-1}\dfrac{c\beta_w - d\tan\theta'}{d\beta_w + c\tan\theta'}$	$\delta_p = 0$
$\tilde{X} = [S\cos\theta'/\cos\theta]e^{i\delta_S}$	$\tilde{X}$ = n.c.
$\tilde{Y} = [S\sin\theta'/\sin\theta]e^{i\delta_S}$	$\tilde{Y}$ = n.c.
$S = (\sqrt{A^2+B^2}/m)\cos\theta$	S = n.c., with $B=0$
$A = \sec\theta' + 2(m-1)\cos\theta' + (a/m)(m-1)^2\sin\theta'$	A = n.c.
$B = (b/m)(m-1)^2\sin\theta'$	$B = 0$

$W \leq 1 (0 \leq \lvert\theta\rvert \leq \theta_{cr})$	$W \geq 1 (\theta_{cr} \leq \lvert\theta\rvert \leq \pi/2)$
$c = D' a/m - F'$	c = n.c.
$d = D' b/m$	$d = 0$
$a/m = (CE + DF)/(C^2 + D^2)$	$a/m = (C' + GF') \div (E' + GD')$
$b/m = (CF - DE)/(C^2 + D^2)$	$b/m = 0$
$C = [(1/6) + 2m/3] \tan\theta'$ $- (\tfrac{1}{2})[(m-1)^2 + (m-1) \div 1.2] \sin 2\theta'$	$C' = (m/3) - 2[1 + (m-1)\cos^2\theta']$
$D = D' \beta_w / \beta^2$	D = not used
$D' = (m-1)[1 + (m-1)\cos^2\theta']$	D' = n.c.
$E = 2 - (m/3) + 2(m-1) \times (\beta_w^2/\beta^2)\cos^2\theta'$	$E' = F'(m-1)/2 - (1 + 2m/3)\tan\theta'$
$F = F' \beta_w / \beta^2$	F = not used
$F' = (m-1)\sin 2\theta'$	F' = n.c.
G = not used	$G = -\tan\theta''$

[Note: Errors have been found in one or the other of the two versions of Ref. 6 from which the preceding expressions are taken or derived; these occur in several equations and in the list of symbols. Those that are applicable have been corrected. Some other errata are corrected in Appendix D of Ref. 21.]

Appendix B: Oblique Shocks

The analysis and results, on a *wavenumber* basis, may be applied to oblique shocks by the usual procedure. The equivalent normal shock transformation

$$M = M_0 \cos\psi \quad \text{or} \quad U_A = U_0 \cos\psi \tag{B1}$$

is made, where M_0 is the upstream Mach number, and ψ is the oblique angle between the shock normal and the upstream flow direction. In Figs. 4 and 5, the designation "1% preshock turbulence" is now to be interpreted as "$(\sin\psi)$% preshock turbulence."

The interpretation of all figures in terms of wavenumber K_1 is unaltered. The proportionality of K_1 to *frequency*, however, does not carry over to the oblique shock case†: Eq. (14) is inapplicable. If K_1 is the component wavenumber along the stream velocity U_0, then Eq. (14) is replaced by

$$\tilde{K}_1 = \omega \tilde{a} L / U_0 \tag{B2}$$

Thus for oblique shocks one-dimensional sprectra should be in terms of $\tilde{K}_1$, not K_1, to be interpreted as frequency spectra. This would entail a rotation of axes (through angle ψ) and a double numerical integration. The appropriate integral is developed, but not evaluated, in Ref. 21.

†An exception is the case of $\Phi_u(K_1)$ for isotropic preshock turbulence.

Acknowledgments

Support at the University of Toronto was aided by a grant from the Natural Sciences and Engineering Research Council of Canada and at NASA Langley Research Center by tenure as a Distinghished Research Associate.

References

[1]Ribner, H. S., "Convection of a Pattern of Vorticity Through a Shock Wave," NACA TN 2864, Jan. 1953; also NACA Rept. 1164, 1954.

[2]Moore, F. K., "Unsteady Oblique Interaction of a Shock Wave with a Plane Disturbance," NACA TN 2879, 1953; also NACA Rept. 1165, 1954.

[3]Kerrebrock, J. L., "The Interaction of Flow Discontinuities with Small Disturbances in a Compressible Fluid," Ph.D. Thesis, California Inst. of Technology, 1956.

[4]Chang, C. T., "Interaction of a Plane Shock and Oblique Plane Disturbances with Special Reference to Entropy Waves," *Journal of the Aeronautical Sciences*, Vol. 24, Sept. 1957, pp. 675-682.

[5]Ribner, H. S. and Tucker, M., "Spectrum of Turbulence in a Contracting Stream," NACA TN 2606, Jan. 1952.

[6]Ribner, H. S., "Shock-Turbulence Interaction and the Generation of Noise," NACA TN 3255, July 1954; also NACA Rept. 1233, 1955.

[7]Batchelor, G. K., *The Theory of Homogeneous Turbulence*, Cambridge University Press, Cambridge, England, 1953, pp. 29 and 49.

[8]Moyal, J. E., "The Spectra of Turbulence in a Compressible Fluid; Eddy Turbulence and Random Noise," *Proceedings of the Cambridge Philosophical Society*, Vol. 48, Pt. 2, April 1952, pp. 329-344.

[9]Grande, E. and Oates, G. C., "Unsteady Flow Generated by Shock-Turbulent Boundary Layer Interactions," AIAA Paper 73-168, 1973.

[10]Trolier, J. W. and Duffy, R. E., "Turbulence Measurements in Shock-Induced Flows," *AIAA Journal*, Vol. 23, Aug. 1985, pp. 1172-1178.

[11]Anyiwo, J. C. and Bushnell, D. M., "Turbulence Amplification in Shock Wave Boundary Layer Interactions," *AIAA Journal*, Vol. 20, July 1982, pp. 893-899.

[12]Zang, T. A., Hussaini, M. Y., and Bushnell, D. M., "Numerical Computations of Turbulence Amplification in Shock-Wave Interactions," *AIAA Journal*, Vol. 22, Jan. 1984, pp. 13-21.

[13]Zang, T. A., Kopriva, D. A., and Hussaini, M. Y., "Pseudospectral Calculation of Shock-Turbulence Interactions," NASA Contractor Rept. 172133, Inst. for Computer Applications in Science and Engineering, NASA Langley Research Center, Hampton, VA, May 1983.

[14]Ram, G. S. and Ribner, H. S., "The Sound Generated by Interaction of a Single Vortex with a Shock Wave," Heat Transfer and Fluid Mechanics Inst., Stanford Univ., 1957, pp. 1-21; also Ribner, H. S., Univ. of Toronto, Inst. for Aerospace Studies, UTIA Rept. 61, 1959.

[15]Ribner, H. S., "Cylindrical Sound Wave Generated by Shock-Vortex Interaction," *AIAA Journal*, Vol. 23, Nov. 1985, pp. 1708-1715.

[16]Hollingsworth, M. A. and Richards, E. J., "On the Sound Generated by the Interaction of a Vortex and a Shock Wave," British Aeronautical Research Council, Rept. 18 257, FM 2371, Feb. 1956.

[17]Dosanjh, D. S. and Weeks, T. M., "Interaction of a Starting Vortex as Well as a Vortex Street with a Traveling Shock Wave," *AIAA Journal*, Vol. 3, Feb. 1965, pp. 216-223.

[18]Pao, S. P. and Seiner, J. M., "Shock Associated Noise in Supersonic Jets," *AIAA Journal*, Vol. 21, May 1983, pp. 687-693.

[19]Tatarski, V. I., *Wave Propagation in a Turbulent Medium*, McGraw-Hill, New York, 1961, p. 5.

[20]Etkin, B., *Dynamics of Atmospheric Flight*, Wiley, New York, 1972, p. 539.

[21]Ribner, H. S., "Spectra of Noise and Amplified Turbulence Emanating from Shock-Turbulence Interaction: Two Scenarios," Univ. of Toronto, Inst. for Aerospace Studies, UTIAS TN 260, March 1986.